IMAGING SYSTEM HAVING WHITE-RGB COLOR FILTER ARRAY

Alexander Getman, Jinhak Kim, Tae-Chan Kim

System LSI Division, Semiconductor Business, Samsung Electronics, Co. Ltd., Republic of Korea

ABSTRACT

We have developed an imaging system comprised of a sensor having White-RGB color filter array and back end image processing chain (IPC) that enables seamless integration with existing imaging solutions.

The key components of our imaging system are 5 megapixel, 1.4um pixel CMOS image sensor covered by White-RGB color filter array and hardware-friendly algorithm which is responsible for conversion of native White-RGB data stream into Bayer RGB and capable to do sharpening and noise suppression simultaneously.

We show that our solution provides artifact free images and outperforms alternative solutions both in terms of visual assessment and SNR improvement.

Index Terms—WRGB image sensor, deconvolution, denoising, interpolation, color restoration.

1. INTRODUCTION

Current trend to increase megapixel count and shrink pixel size of color image sensor results in substantial degradation of sensitivity. Among methods to alleviate this problem several strategies have been developed including improvement image processing and optimization of color filter array (CFA).

A majority of color image sensors nowadays utilize mosaic CFA that was first introduced by Bayer [1] (Fig.1a). This CFA is formed by primary colors and has twice as many green pixels as red or blue to reflect the fact that human eye has better sensitivity to green band of visible spectrum. In spite of the fact that this pattern is well studied and widely adopted, it is often criticized for having high amount of light energy being absorbed by color filter material [2]. Recently, a series of publications have been devoted to development of more transparent CFA alternative to Bayer [2,3,4].

An interesting idea to design CFA in Fourier domain was proposed by Hirokawa, et.al. [3]. According to the authors, a CFA designed in such a way is capable to greatly reduce color aliasing and noise. Nevertheless, large elementary cell of such CFA (Fig. 1c,d)) as well as sophisticated image interpolation and color processing procedure that is different from the conventional approach represent a challenge to practical implementation.

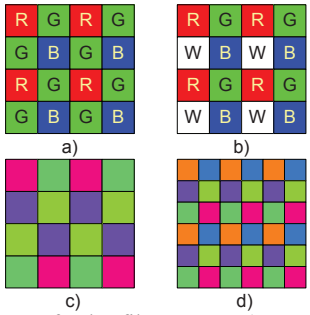

Fig. 1 Various types of color filter arrays. a) Bayer CFA [1], b) White-RGB CFA [2], c) CFA proposed by Hirakawa, et.al [3], d) CFA proposed by Condat [4].

A White-RGB CFA presented in [2] is interesting for two aspects. First, it contains pixels of all three primary colors and differs from conventional Bayer CFA by only one pixel (Fig. 1b). This property enables very efficient implementation of image processing chain (IPC). Second, insertion of white filter makes CFA more transparent than Bayer's and should improve image quality at poor illumination with minimal impact on color reproduction.

Taking into account simplicity of implementation and potential to provide improved sensitivity we have decided to investigate imaging system having White-RGB CFA in more details. The layout of rest of the paper is as follows. The second section explains structure of our IPC required for processing of White-RGB data stream, third section demonstrates performance of our imaging system, and final section draws a conclusion.

2. WHITE-RGB IMAGING SYSTEM

The White-RGB imagines system described herein consists of two major parts: image sensor having White-RGB CFA and back end image processing circuit.

The image sensor having 5 megapixel resolution and 1.4um pitch was fabricated using standard CMOS technology. The sensor was covered by CFA shown on Fig. 1b). The color pigments used in this CFA were identical to ones used in fabrication of Bayer CFA. White pixel was obtained by skipping deposition of color pigment. Resultant spectral quantum efficiency (QE) plot is shown on Fig.2. As one may observe, the spectral sensitivity curves of each color channel have irregular shapes which strongly overlap with each other. This implies that image obtained by such

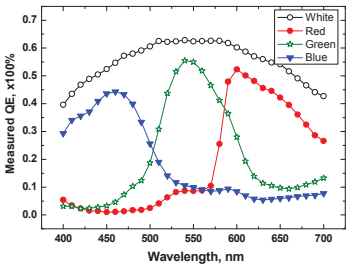

Fig. 2 Measured quantum efficiency of the White-RGB sensor.

sensor will require strong color restoration and "intuitive" color relations like those shown by equation (1) are not valid.

$$White = Red + Green + Blue \quad (1)$$

The back-end image processing circuit is responsible for noise suppression and conversion of native White-RGB data stream into the Bayer one. Such architecture allows us to seamlessly integrate our sensor with existing imaging solutions based on Bayer CFA. Another inherent feature of the back-end processing is sharpening, so it becomes possible to correct lens aberrations and sharpen image without enhancing noise. The overall scheme of our White-RGB system is shown on Fig.3

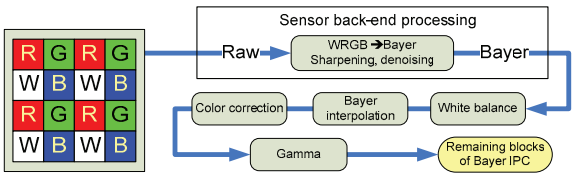

Fig. 3 Block-scheme of White-RGB system.

In order to implement efficient White-RGB back-end IPC one should solve these issues:

1) How to utilize information from "White" pixel.
2) How to prevent image artifacts when one of the color channels (especially "White") saturates.
3) How to take into account non-ideal spectral sensitivity that breaks "intuitive" color relations.

Analysis of previously published results reveals that methods [2, 5] based on the color separation process given by equation (2) are not capable to solve issues 2 and 3 mentioned above.

$$G_W = W \cdot \frac{G_{average}}{R_{average} + G_{average} + B_{average}} \quad (2)$$

Let us consider the color separation equation (2) that provides a way to estimate value of the "Green" pixel at the position of "White" during White-RGB to Bayer conversion. If color relation equation (1) is not valid, we should expect that estimate G_W will deviate from true "Green" pixel signal, resulting in a strong grid-pattern noise. Moreover, levels of illumination, when estimated G_W and true "Green" pixels saturate, are very different. The resultant image artifacts caused by disparity of true and restored green signals are unacceptable (See Fig. 6).

It was reported before that interpolation technique based on linear filtering is very flexible and can provide high-quality results [3,4,6]. In case of White-RGB processing problem linear estimator of G_W is given by

$$G_{W\,mn} = \sum_{ij=-M..M} \alpha_{ij} \cdot X_{i+m,j+n}, \quad (3)$$

where $G_{W\,mn}$ is the estimated G_W pixel with coordinates (m, n), $X_{i+m,j+n}$ is the local window of image sampled by WRGB CFA that have size $(2M+1)\times(2M+1)$ and center coordinates $(i+m, j+n)$ and α_{ij} are tunable filter coefficients determined by sensor spectral QE, layout of color filter array and other camera parameters. A remarkable property of equation (3) is that one may find a set of coefficients α_{ij} that will make estimate G_W immune to saturation of "Blue", "Red" or "White" channels while exploiting cross-channel correlation when these signals are not saturated. This can be achieved by making estimate G_W independent from local-average values of non-green color channels. Equation (3) in this case can be replaced by a constrained linear estimator:

$$G_W = f(G) + Hp_1(R) + Hp_2(B) + Hp_3(W), \quad (4)$$

where $Hp(\cdot)$ means high-pass local linear filter and $f(\cdot)$ is a not constrained linear function.

Although equation (4) can solve all three aforementioned issues, better results and functionality are achievable when some noise cancellation precedes linear estimation process. For example, equation (3) or (4) can be used for sharpening of the image and compensation of lens blur if applied for all color channels. In the later case, noise cancellation will prevent from excessive amplification of noise during linear filtering and improve reproduction of high-frequency details as discussed in [7, 8].

Wavelet based denoising is an ideal choice for back-end IPC because it allows processing of the whole window while substantially reducing memory footprint. Our back-end IPC uses a shift-invariant redundant Haar wavelet transform [9, 10] with 4 levels of decomposition (2 levels in horizontal and 2 levels in vertical direction). This type of wavelet transform is very efficient in implementation in hardware as a feed-forward sequence of summations and subtractions.

During wavelet denoising step we intentionally avoid separate processing of different color channels. This enables us to more efficiently utilize cross-channel correlation and use information from low-noise "White" color channel during restoration of remaining "Red", "Green" and "Blue".

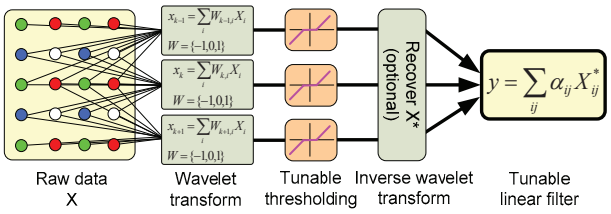

Fig. 4 Structure of back-end IPC for Whit-RGB to Bayer conversion.

Fig. 4 summarizes mathematical model of back-end IPC described above. For the sake of simplicity we will refer to the proposed algorithm as Universal Restoration Algorithm (URA). This diagram also shows that URA resembles Tunable Threshold Network (TTN) algorithm [11, 12] and Wavelet-Vaguelette Decomposition described in [8].

The size of input window X used by URA algorithm is flexible and depends upon application. The results presented in this work were obtained using 9 by 9 pixel window.

The effectiveness of the proposed algorithm strongly depends upon selection of tuning parameters (i.e. thresholds of the wavelet denoising and coefficients of linear filter) and simplicity of finding their optimal values.

Due to the complexity of the tuning problem, explicit evaluation of parameters for URA is intractable. For this reason, we have decided to adopt supervised learning technique [13] widely used for neuron network training. The goal of the supervised learning is to find such set of tuning parameters that when the observation image is processed by the URA the resultant image is as close as possible to the desirable target image. It is a common practice to estimate the difference between the resultant and target images using mean square error (MSE). If such tuning parameters are found we may expect that any input image similar to the observation image should be restored correctly.

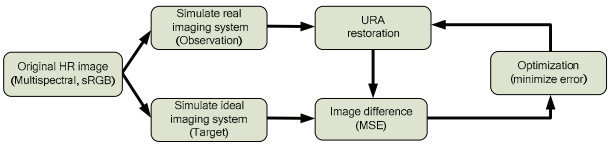

Fig. 5 Schematic structure of tuning procedure. The algorithm is tuned to minimize difference between the target and observation using a cost function such as MSE.

Our tuning procedure requires two images. The first image represents the input of the URA (observation image) and the second image represents the desired output, which the URA should produce (target image). We will refer to this pair of images as a training pair. We obtain both images of the training pair from some original high-resolution image through simulation process. Thus, in order to get observation image we should simulate all processes of image formation occurring in White-RGB imaging system including noise, lens blur, QE response and pixel sampling according to White-RGB CFA. In contrast, the target image should represent image that has no lens blur, no noise and pixel sampling according to Bayer CFA. The diagram illustrating the tuning procedure is shown on Fig. 5.

3. EXPERIMENTAL RESULTS

In order to demonstrate performance of the proposed White-GRB imaging system we have prepared a series of experiments[1]. The images presented here were obtained using the sensor and back-end IPC described in previous chapter. Resultant Bayer output was processed by the image pipeline, shown on Fig. 3.

Our first experiment will demonstrate behavior of our White-GRB imaging system when some color channel saturates. The saturation was realized by overexposure of the captured scene. We have implemented a White-RGB to Bayer converter based on color separation process (2) as a reference point. Final images are shown on Fig. 6. We can identify that under overexposure conditions color separation process fails to correctly reproduce colors and high-frequency details (yellow patch and text on the Fig. 6, right) There is no such artifacts on the image produced by the proposed URA back-end IPC.

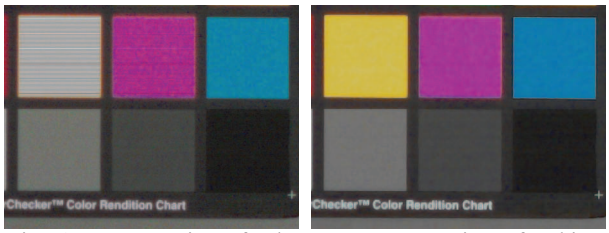

Fig. 6 Demonstration of robustness to saturation of White-RGB system. Output of the reference color separation IPC based on (2) is shown on left and output of the proposed URA IPC is shown on right.

Our second experiment compares resolution performance of the proposed White-RGB and Bayer imaging systems. In order to isolate CFA related effects both imaging systems were using identical imaging lenses, pixel structures, captured scene composition and exposure settings. White-RGB image was processed by IPC shown on Fig.3 where back-end processing was tuned to do denoising, sharpening and pixel stream converting while Bayer image was processed by the same IPC where back-end part was disabled.

According to the paradigm of pixel stream conversion, resolution performance of the White-RGB system can't exceed that of Bayer. Fig. 7 illustrates strength of this effect.

[1] Paper with color version of images is available online.

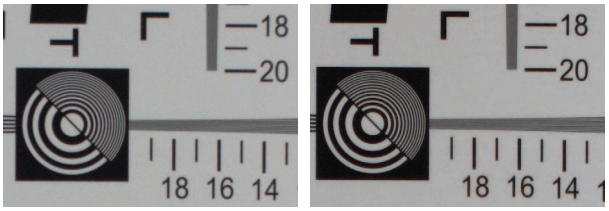

Fig.7 Comparison of resolution performance. Conventional Bayer system is shown on left and proposed White-RGB system is shown on right.

Experimental results do confirm marginal resolution loss. Nevertheless, White-RGB image is clean and has sharp appearance that is more preferable. Please note that these images were post-processed by a "color correction" and "gamma" as shown on Fig. 3. This means that false color artifacts and noise are strongly amplified on these images.

Our final experiment compares SNR performance and demonstrates appearance of natural image captured with White-RGB system. The capturing conditions were similar to those of previous experiment. The SNR was measured as standard deviation of pixels on patch #22 of Macbeth chart having neutral gray color. The resultant image is shown on Fig.8 and SNR values are summarized in Table 1.

Table 1
SNR Performance comparison

Sensor type	Luminance dB	Red dB	Green dB	Blue dB
Bayer	**28.4**	**26.2**	**27.1**	**25.0**
White-RGB	**33.0**	**31.5**	**31.5**	**31.0**


Fig.8 "Studio" image captured with the proposed White-RGB system.

4. CONCLUSION

We have presented fully functional White-RGB imaging system that includes image sensor and back-end IPC. The core of the IPC is the Universal Restoration Algorithm responsible for proper use of signal captured by "White" pixel provides additional functionalities such as denoising and sharpening. Unlike alternative approaches based on color separation process (2) URA has robust behavior in overexposed images and is capable to recover image data from sensors having non-ideal spectral sensitivity of color channels. According to the experimental results, our solution is comparable to conventional Bayer system in terms of resolution, has better SNR and provides artifact-free images. Feed-forward architecture of URA and wavelet denoising based on Haar wavelet transform enable efficient implementation of the algorithm in hardware.

5. REFERENCES

[1] B. E. Bayer, "Color imaging array," *US Patent 3971065*, 1976.
[2] H. Honda et al., "A novel Bayer-like WRGB color filter array for CMOS image sensors", *Electronic Imaging*, 2007.
[3] K. Hirakawa and P. J. Wolfe, "Spatio-spectral color filter array design for optimal image recovery," *IEEE Trans. Image processing*, vol. 17, no. 10, pp. 1876–1890, Oct. 2008.
[4] L. Condat, "A new colour filter array with optimal sensing properties," *IEEE ICIP*, Nov. 2009, Cairo, Egypt
[5] "Solid-State Image-Pickup Device having primary color and gray color filters and processing means thereof", *US Patent 7126633*, 2006.
[6] Malvar, et. al., "High-quality linear interpolation for demosaicing of Bayer-patterned color images", *ICASSP*, 2004.
[7] R.Neelamani, et. al., "ForWaRD: Fourier-wavelet regularized deconvolution for ill-conditioned systems", *IEEE Transactions on Signal Processing*, 2004.
[8] D.L. Donoho, "Nonlinear solution of linear inverse problems by wavelet-vaguelette decomposition," *Appl. Comput. Harmon. Anal.*, vol. 2, pp. 101–126, 1995.
[9] R.R. Coifman, D.L. Donoho, "Translation-invariant de-noising", in: A. Antoniadis, G. Oppenheim (Eds.), Wavelet and Statistics, Lecture Notes in Statistics, Springer, Berlin, pp. 125–150, 1995.
[10] Sahracian, et. al., "An Improved Image Denoising Technique Using Cycle Spinning", *ICT-MICC*, 2007.
[11] Xiao-Ping Zhang, "Space-scale adaptive noise reduction in images based on thresholding neural network," *Proceedings of the Acoustics, Speech, and Signal Processing*, 2001.
[12] M. Nasri, et. al., "Image denoising in the wavelet domain using a new adaptive thresholding function," *Neurocomputing*, vol. 72, Issues 4-6, 2009.
[13] S. Kotsiantis, "Supervised Machine Learning: A Review of Classification Techniques", *Informatica* Journal 31, 2007
[14] S. Kawada, at. al., "A wide dynamic range checkered-color CMOS image sensor with IR-Cut RGB and visible-to-near-IR pixels" ; Sensors, 2009 IEEE , Page(s): 1648 - 1651